IMPACT MECHANICS – CASE STUDY 1:

CALIBRATION OF CONSTITUTIVE RELATIONS AND FAILURE CRITERIA FOR IMPACT PROBLEMS

Problem:

In this case study elastic-thermoviscoplastic constitutive relations and proper failure criteria for uncoupled simulations of impact problems will be calibrated and validated based on mechanical tests and numerical simulations. Two different versions of the well-known and much used Johnson-Cook constitutive relation will be applied, while failure will be modelled using two different uncoupled damage models (see also [1]). For both models the constitutive behaviour is assumed to be isotropic and modelled with J_2 plasticity. In addition, simulations using a porous plasticity model should be carried out and compared to the experimental data and the uncoupled damage models.

Firstly, the original Johnsen-Cook constitutive relation [2] and fracture criterion [3], available in Abaqus/Standard and Abaqus/Explicit, will be considered. The viscoplastic constitutive relation valid in the plastic domain is given as

$$\sigma_{eq} = \left(A + Bp^n\right)(1 + C \ln \dot{p}^*)(1 - T^{*m}) \tag{1}$$

where $\sigma_{eq} = \sqrt{\frac{3}{2}\sigma'_{ij}\sigma'_{ij}}$ is the von Mises equivalent stress, p is the equivalent plastic strain and $\left(A, B, n, C, m\right)$ are model constants. The dimensionless plastic strain rate is given by $\dot{p}^* = \dot{p}/\dot{p}_0$ where $\dot{p}_0$ is a user-defined reference strain rate. The homologous temperature is defined as $T^* = \left(T - T_0\right)/\left(T_m - T_0\right)$, where T is the absolute temperature, T_0 is the reference temperature and T_m is the melting temperature of the material. The Johnson-Cook fracture criterion is given as

$$\omega = \int_0^p \frac{dp}{p_f} \le 1 \quad , \quad p_f = \left[D_1 + D_2 \exp\left(-D_3\sigma^*\right)\right]\left(1 + D_4 \ln \dot{p}^*\right)\left(1 + D_5 T^*\right) \tag{2}$$

where ω is the damage, p_f is the fracture strain, $\sigma^* = \sigma_H / \sigma_{eq}$ is the stress triaxiality where σ_H is the hydrostatic stress, and $\left(D_1, D_2, D_3, D_4, D_5\right)$ are model constants. Note that the constant D_3 is given as negative in the Abaqus implementation of the model, while in the original model it is given as positive.

Secondly, a modified version of the Johnson-Cook (MJC) constitutive relation [4] available in the SIMLab Metal Model (SMM) should be calibrated. The viscoplastic constitutive relation is now expressed as

$$\sigma_{eq} = \left(\sigma_0 + \sum_{i=1}^{2} Q_{Ri}\left(1 - \exp\left(-C_{Ri}\, p\right)\right)\right)(1 + \dot{p}^*)^C (1 - T^{*m}) \tag{3}$$

where $(\sigma_0, Q_{R1}, C_{R1}, Q_{R2}, C_{R2}, C, m)$ are model constants. Failure is modelled using a criterion proposed by Cockcroft and Latham (CL) [5]

$$\omega \equiv \frac{1}{W_C}\int_0^p \langle \sigma_I \rangle \mathrm{d}p = \omega = \frac{1}{W_C}\int_0^p \left\langle \sigma^* + \tfrac{2}{3}\cos\theta_L \right\rangle \sigma_{VM}\, dp \tag{4}$$

where W_C is the fracture parameter. Further, σ_I is the maximum principal stress, $\langle \sigma_I \rangle = \sigma_I$ when $\sigma_I \geq 0$ and $\langle \sigma_I \rangle = 0$ when $\sigma_I < 0$, while θ_L is the Lode angle and σ_{VM} is the equivalent von Mises stress. As seen, failure cannot occur for the CL fracture criterion when there are no tensile stresses operating.

For both models the temperature change due to adiabatic heating is calculated as

$$T = T_0 + \Delta T \quad , \quad \Delta T = \int_0^p \beta \frac{\sigma_{eq} dp}{\rho c_\varepsilon} \tag{5}$$

where ρ is the material density, c_ε is the specific heat and β is the Taylor-Quinney coefficient that represents the proportion of plastic work converted into heat. In this case study we will assume $m = 1$ (linear decrease of equivalent stress with increasing temperature).

The high strength steel Weldox 700E from SSAB will be considered in the following. Weldox 700E is a structural steel that goes through a significant quenching and tempering (QT) process. Table 1 gives the chemical composition of the material, while Figure 1 shows the microstructure. Weldox 700E consists of tempered martensite that indicates high strength but also low ductility. In order to make the alloy more ductile, the martensite has been exposed to tempering. This microstructure consists of small ball-shaped particles of iron-carbide, which have been precipitated between the martensite needles. Some of the lattice stresses due to the quenching process are released and this causes an increase in ductility. The high strength is kept through the fine iron-carbides precipitation.

Table 1. Chemical composition (weight %) of Weldox 700 E.

C	Si	Mn	P	S	B	Nb	Cr	V	Cu	Ti	Al	Mo	Ni	N
0.20	0.6	1.6	0.020	0.010	0.005	0.04	0.7	0.09	0.3	0.04	0.015	0.70	2.0	0.015

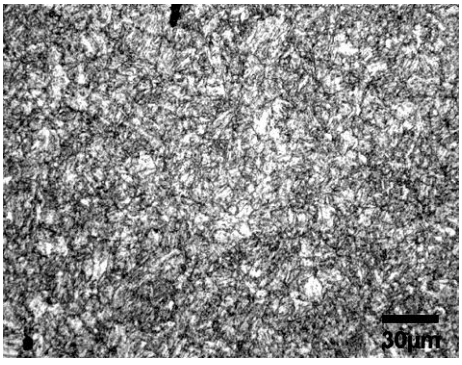

Figure 1: Microstructure of the Weldox 700E steel.

In order to calibrate the two different versions of the Johnson-Cooks model given in Equation (1) and Equation (3), material tests involving large strains, high strain rates and high temperatures have to be performed. Only the two former will be considered in this case study, while the thermal effects will be estimated.

We start by doing quasi-static tensile tests on smooth axisymmetric specimens taken from the rolling direction of the steel plate. The geometry of the specimen can be found in Figure 2 (a). The tension tests will be conducted in a 20 kN DARTEC servo-hydraulic universal testing machine at a strain rate of 5×10^{-4} s^{-1}. During testing, the diameter at minimum cross-section of the specimen is continuously measured until fracture. This is made possible using an in-house measuring rig with two perpendicular lasers that accurately measures the specimen diameter (see Figure 2 (b)). Each laser projects a beam with dimension 13×0.1 mm^2 towards the detector on the opposite side of the specimen. Thus, the two orthogonal lasers create a box of laser light of $13 \times 13 \times 0.1$ mm^2 around the minimum cross-section of the sample. As the specimen is deformed, the continuous change in diameters is observed by the detectors. This dual-axis micrometre is made up of a high-speed, contact-less AEROEL XLS13XY laser gauge with 1 μm resolution. The gauge is installed on a mobile frame to ensure that the diameters always are measured at minimum cross-section. During elongation, the sample is scanned at a frequency of 1200 Hz and the measured data is transferred by the built-in electronics to the remote computer via fast Ethernet. The diameters are measured in the thickness direction of the plate (x) and in the transverse direction of the specimen (y), denoted D_x and D_y respectively.

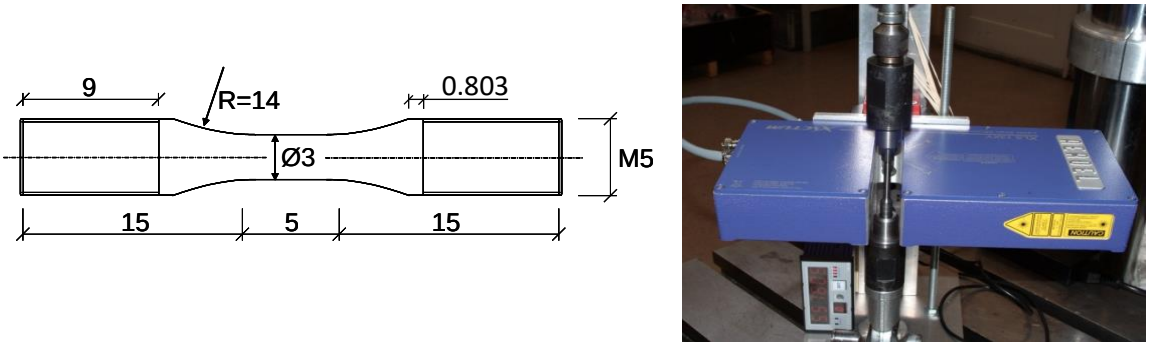

(a) (b)

Figure 2: (a) Geometry of test specimen (measures in mm) and (b) picture of laser gauge.

Outputs from these tests include the force F and the continuous measurements of the diameter reduction in two perpendicular directions. Based on these measurements the average Cauchy (true) stress and the logarithmic (true) strain are calculated as

$$\sigma_t = \frac{F}{A} \quad \text{and} \quad \varepsilon_l = \ln\frac{A_0}{A} \tag{6}$$

where F is the force, $A_0 = \frac{\pi}{4} D_0^2$ is the initial cross-section area, and D_0 is the initial diameter of the gauge section. The current area of the cross section is assumed to be elliptical and obtained as

$$A = \frac{\pi}{4} D_x D_y \tag{7}$$

The formation of a neck in the tensile specimen at large strains introduces a complex triaxial stress state in that region by producing radial and transverse stresses which raise the value of

the longitudinal stress required to cause plastic flow. In other words, the measured longitudinal true stress needs to be corrected for triaxiality effects, since this stress is not equal to the equivalent stress after necking. The equivalent stress after necking can be obtained using Bridgman's analysis and Le Roy's empirical model, i.e.,

$$\sigma_{eq} = \frac{\sigma_t}{(1+2R/a)\ln(1+a/2R)} \tag{8}$$

$$a/R = 1.1(p-\varepsilon_{lu}^{p}) \ , \ \ p > \varepsilon_{lu}^{p} \tag{9}$$

where σ_{eq} is the equivalent stress, p is the equivalent plastic strain, ε_{lu}^{p} is the logarithmic plastic strain at necking, a is the radius of the current cross-section of the specimen and R is the radius of the curvature of the neck

A Split-Hopkinson tension bar (SHTB) will be employed in the tests with strain rates higher than 100 s^{-1}. A principle sketch of the SHTB is shown in Figure 3. The rig consists of two steel bars with lengths of about 8 and 7 m, and a circular cross section with diameter 10 mm. The test specimen is mounted between the bars. Before the test, a locking mechanism clamps point B, and part AB of the bar is pre-stretched. A tension stress wave $\varepsilon_I(t)$ propagates towards point C when the clamp at B suddenly is removed. This wave is partly reflected as $\varepsilon_R(t)$, i.e., a wave travelling back to A, and partly transmitted as $\varepsilon_T(t)$, i.e., a wave propagating into the specimen and further into bar DE. The specimen is normally strained to fracture during this transmission process.

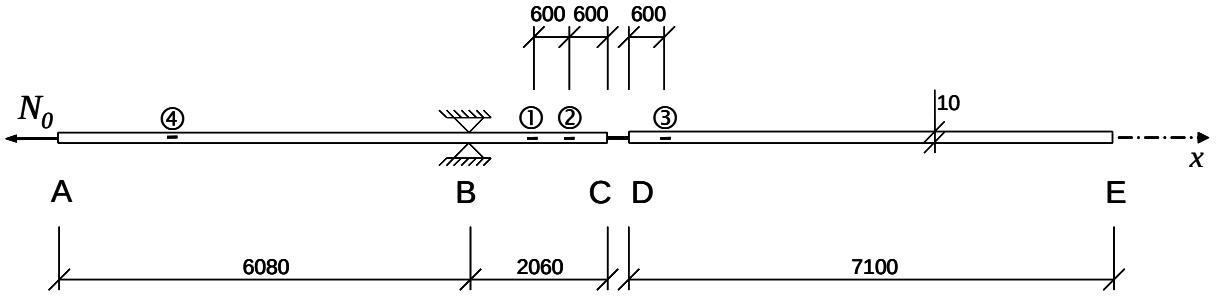

Figure 3: Principal overview of the SHTB at SIMLab (measures in mm).

With use of stress-wave propagation theory, the nominal stress, nominal strain and mean nominal strain rate in the specimen can be calculated based on the strain gauge registrations at points 2 and 3 as

$$\sigma_e(t) = \frac{E_b A_b}{A_s}\varepsilon_T(t) \tag{10}$$

$$\varepsilon_e(t) = -2\frac{c}{L_s}\int_0^t \varepsilon_R(t)dt \tag{11}$$

$$\dot{\varepsilon}_e(t) = -2\frac{c}{L_s}\varepsilon_R(t) \tag{12}$$

Here subscripts b and s refer to the bar and specimen, respectively. The stress wave propagation velocity is given as $c = \sqrt{E_b/\rho_b}$, where E_b is Young's modulus and ρ_b is the density of the bars. A_s is the cross-section area and L_s is the length of the specimen's parallel section, i.e., $L_s = 5$ mm in our case. Based on Equations (10) and (11), the true stress and strain until necking may be found as

$$\sigma_t(t) = \left(1+\varepsilon_e(t)\right)\sigma_e(t) \tag{13}$$

$$\varepsilon_l(t) = \ln\left(1+\varepsilon_e(t)\right) \tag{14}$$

while the true plastic strain is found as $\varepsilon_l^p(t) = \varepsilon_l(t) - \varepsilon_l^e(t) = \varepsilon_l(t) - \sigma_t(t)/E$. Further details regarding the experimental set-up and the processing of the results are provided in Clausen et al. [6][7] and Langseth and Clausen [8], where also an analytical solution of the SHTB-equations given above are provided.

Tasks:

1) Show that the modified Johnson-Cook (MJC) model presented in Equation (3) fulfils the requirements of a multiplicative thermoviscoplastic constitutive relation.

2) Quasi-static tension tests using the axisymmetric specimen shown in Figure 2 (a) will be conducted. During testing, the laser gauge presented in Figure 2 (b) will be applied to measure the diameter reduction of the specimen at minimum cross section until fracture. Based on these measurements, establish force – diameter reduction curves and true stress – true plastic strain curves. Is it reasonable to assume the material as isotropic, or is there anything in the test that indicates that the material is anisotropic?

3) Determine the logarithmic plastic strains at necking. The strain at failure should also be explicitly stated. Use Bridgman's analysis and Le Roy's empirical model to calculate the equivalent stress – equivalent plastic strain curve.

4) Use a spreadsheet, MATLAB or similar to conduct a direct calibration of the material constants for the constitutive relations in Equation (1) and Equation (3), and for the CL fracture criterion in Equation (4). We do not have sufficient material data to calibrate the JC fracture criterion given in Equation (2) in this case study, so these data are taken from Dey [9]. Physical constants required for numerical simulations should be found from the literature. Note also that relevant material constants are given in the file "Calibration steps" in the folder "Case Studies/Case Study 1" on Blackboard. Plot and compare the results with the experimental data.

5) Establish a 2D axisymmetric element model in Abaqus of the material test specimen in Figure 2 (a). Use the material data provided in Task 4), and validate that you are able to reproduce the quasi-static stress-strain curve, the necking and the failure in the specimen.

Are there any differences in results between the JC and the MJC models? Both implicit and explicit simulations should be carried out. If the results are not satisfactory, use trial and error (especially on the failure criteria) to tune the material constants in an attempt to increase the accuracy.

6) Dynamic tension tests using the axisymmetric specimen shown in Figure 2 (a) will be conducted in the SHTB. 3-4 tests at various strain rates should be carried out. Establish the engineering stress-strain curves at elevated strain-rates, and plot the true stress versus the true plastic strain rate for different values of plastic strain (e.g. 2%, 4% and 6%). Use this to determine the strain-rate sensitivity constant C in the constitutive models.

7) Use the same 2D axisymmetric element model of the material test specimen as in Task 5). Run simulations of the dynamic tests and compare the results to the experimental data. Both isothermal and adiabatic conditions should be considered. Tune the material properties if required. What can be done to improve the results?

8) Voluntary: The Gurson model is a much-used porous plasticity model. It is given as

$$f = \frac{\sigma_{eq}^2}{\sigma_M^2} + 2\omega\beta_1 \cosh\left(\frac{\beta_2\sigma_{kk}}{2\sigma_M}\right) - 1 - \beta_3\omega^2 = 0 \qquad (15)$$

where typical values for $\beta_1, \beta_2, \beta_3$ are $3/2, 1, 9/4$, respectively, ω is the porosity, σ_M is the flow stress of the matrix material and σ_{eq} is the equivalent macroscopic von Mises stress. Run the quasi-static tensile test from Task 2) using the model in Task 5) and the Gurson model (called "porous metal plasticity" in Abaqus). Note that in Abaqus the porosity is introduced through the relative density, given as $\rho = 1 - \omega$. Use the same parameters as for the MJC criterion in Equation (3), but add the keyword "*porous metal plasticity" in the material card instead of the "*user defined field" keyword. The porous metal plasticity keyword is used to introduce the GTN parameters β_1, β_2 and β_3 as well as the relative density:

*porous metal plasticity, relative density=rho
beta1, beta2, beta3

An alternative approach in the standard version of Abaqus would have been to use the same elastic constants as in Task 5) and to tabulate the strain hardening (can be done under "plasticity" in Abaqus) based on the calibration of the MJC criterion in Equation (3).

Run simulations with 3 different values of ω (e.g. $\omega_1 = 0.001$, $\omega_2 = 0.01$ and $\omega_3 = 0.1$). Compare the results to those from Task 4) and 5). Note that in order to visualize the void volume fraction, the field output VVF must be requested.

9) A report of maximum 10 pages should be worked out based on the tasks presented above.

References

[1] Hopperstad OS, Børvik T. Modelling of plasticity and failure with explicit finite element methods, Lecture Notes in TKT 4128 Impact Mechanics, SIMLab/Department of Structural Engineering, NTNU, 2017.

[2] Johnson GR, Cook WH. A constitutive model and data for metals subjected to large strains, high strain rates and high temperatures. In: Proceedings of the 7th International Symposium on Ballistics. 1983, p. 541-547.

[3] Johnson GR, Cook WH. Fracture characteristics of three metals subjected to various strains, strain rates, temperatures and pressures. Engineering Fracture Mechanics 1985; 21; 31-48.

[4] Børvik T, Hopperstad OS, Berstad T, Langseth M. A computational model of viscoplasticity and ductile damage for impact and penetration. European Journal of Mechanics – A/Solids 2001; 5; 685-712.

[5] Cockcroft MG, Latham DJ. Ductility and the workability of metals. Journal of the Institute of Metals 1968; 96; 33-39.

[6] Clausen AH, Auestad T. Split-Hopkinson Tension Bar. Experimental Set-up and Theoretical Considerations. SIMLab Report R-16-02, NTNU, 2002.

[7] Clausen AH, Auestad T, Langseth M. A Split-Hopkinson Tension Bar including High-Temperature Testing Facilities. SIMLab Report, NTNU, 2005.

[8] Langseth M, Clausen A, Børvik T. Impact and Energy Absorption, Lecture Notes in TKT 4128 Impact Mechanics, SIMLab/Department of Structural Engineering, NTNU, 2016.

[9] Dey S. High-strength steel plates subjected to projectile impact. PhD-thesis 2004:38, NTNU, 2004.